Quantification of molecular interactions between ApoE, amyloid-beta (Aβ) and laminin: Relevance to accumulation of Aβ in Alzheimer's disease

Quantification of molecular interactions between apoE, Amyloid-beta (Aβ) and laminin: Relevance to accumulation of Aβ in Alzheimer's disease

Jurgita Zekonyte[1*#], Kenji Sakai[2], James A. R Nicoll[3], Roy O Weller[3], Roxana O Carare[3]

[1] Faculty of Engineering and Environment, University of Southampton, UK

[2] Department of Neurology, Kanazawa University Hospital, Kanazawa, Japan

[3] Faculty of Medicine, University of Southampton, UK

* Corresponding Author

Dr. Jurgita Zekonyte

School of Engineering

University of Portsmouth

Anglesea Building, A1.06d

Anglesea Road

Portsmouth PO1 3DJ

Tel: +44 (0)23 9284 2330

e-mail: Jurgita.Zekonyte@port.ac.uk

Abstract

Accumulation of amyloid-β (Aβ) in plaques in the brain and in artery walls as cerebral amyloid angiopathy indicates a failure of elimination of Aβ from the brain with age and Alzheimer's disease. A major pathway for elimination of Aβ and other soluble metabolites from the brain is along basement membranes within the walls of cerebral arteries that represent the lymphatic drainage pathways for the brain. The motive force for the elimination of Aβ along this perivascular pathway appears to be the contrary (reflection) wave that follows the arterial pulse wave. Following injection into brain parenchyma, Aβ rapidly drains out of the brain along basement membranes in the walls of cerebral arteries; such drainage is impaired in apolipoprotein E ε4 (ApoE4) mice. For drainage of Aβ to occur in a direction contrary to the pulse wave some form of attachment to basement membrane would be required to prevent reflux of Aβ back into the brain during the passage of the subsequent pulse wave. In this study, we show first that apolipoprotein E co-localizes with Aβ in basement membrane drainage pathways in the walls of arteries. Secondly, we show by Atomic Force Microscopy that attachment of ApoE4/Aβ complexes to basement membrane laminin is significantly weaker than ApoE3/Aβ complexes. These results suggest that perivascular elimination of ApoE4/Aβ complexes would be less efficient than with other isoforms of apolipoprotein E, thus endowing a higher risk for Alzheimer's disease. Therapeutic correction for ApoE4/Aβ/laminin interactions may increase the efficiency of elimination of Aβ in the prevention of Alzheimer's disease.

Keywords: Apolipoprotein E, perivascular clearance pathways, laminin, atomic force microscopy, amyloid-β. Cerebral amyloid angiopathy, Alzheimer's disease

1. Introduction

A key feature of Alzheimer's disease pathology is the extracellular accumulation of soluble amyloid-β (Aβ) and of insoluble Aβ as plaques in brain parenchyma and in the walls of cerebral arteries as cerebral amyloid angiopathy (CAA) [1, 2]. These features indicate that there is a failure of elimination of Aβ from the brain with increasing age and in Alzheimer's disease [3]. Mechanisms for elimination of Aβ from the brain include enzymatic degradation by neprilysin within brain tissue and artery walls; absorption of Aβ into the blood mediated by low density lipoprotein receptor-1 and elimination by lymphatic drainage along basement membranes in the walls of cerebral capillaries and arteries [4]. Accumulation of insoluble fibrillar Aβ in the walls of capillaries and arteries in CAA reflects failure of elimination of Aβ along lymphatic drainage pathways with age and Alzheimer's disease [5].

When soluble tracers, including Aβ, are injected into the brain parenchyma, they are rapidly eliminated along basement membranes of capillaries towards cervical lymph nodes [6, 7]. The pattern of deposition of Aβ in the walls of capillaries and arteries in human CAA exactly mirrors the lymphatic drainage pathways defined in experimental tracer studies [5]. Tracers and Aβ appear to leave the walls of the carotid artery in the neck at the level of cervical lymph nodes as they drain from the brain to regional lymph nodes in the neck [6, 8]. Perivascular drainage of Aβ from the brain is impaired with age as shown experimentally and by the presence of CAA in aging humans [9]. Aβ secreted by amyloid precursor protein (APP)-transgenic mice harboring the Swedish double mutation driven by a neuron specific promoter is observed in the perivascular drainage pathways as CAA co-localized with apolipoprotein E (ApoE) [1]. Furthermore, perivascular drainage of Aβ is impaired in mice expressing human apolipoprotein E ε4 (ApoE4) suggesting that the risk factor for Alzheimer's disease in patients possessing the ε4 allele of ApoE may be related to a failure of elimination of Aβ from brain [10].

Studies on the motive force for perivascular drainage of Aβ from the brain suggest that solutes are driven along basement membranes in the walls of arteries by the contrary (reflection) wave that follows the pulse wave [11]. In order for this mechanism to function effectively, some form of attachment of transported material to basement membrane proteins would be required in order to prevent reflux of material during passage of the pulse wave itself. If no attachment activity were present, Aβ and other solutes would oscillate within the basement membrane rather than be driven rapidly out of the brain as has been observed experimentally. One of the major candidates for performing such attachment activity for Aβ is ApoE.

ApoE is the predominant lipoprotein in the brain and regulates transport of cholesterol from astrocytes to neurons [12-14]. Three *APOE* alleles (ε2, ε3 and ε4) encode the production of corresponding protein isoforms (E2, E3 and E4). Binding of Aβ to ApoE has been proposed as a mechanism by which Aβ is transported across the blood-brain barrier [4] and levels of ApoE are lower in ApoE4-positive individuals than in ApoE3 carriers [15]. Recent work has demonstrated minimal direct physical interaction between ApoE and soluble Aβ within the cerebrospinal fluid [16]. Thus, the role of ApoE in mediating the clearance of Aβ from the brain remains unresolved.

Since Aβ40 is the predominant type of Aβ found in CAA [17], in the present study we tested the hypothesis that interactions of Aβ40 with protein components of cerebral vascular basement membranes, such as laminin, are stronger in the presence of ApoE3 than in the presence of apoE4. If this hypothesis is substantiated, it would suggest that perivascular drainage of Aβ in individuals possessing ApoE4 would be less efficient due to defective attachment of Aβ/ApoE4 complexes to basement membranes during perivascular lymphatic drainage. This would ultimately lead to failure of elimination of Aβ from the brain and its deposition in artery walls as CAA. .

In order to test the hypothesis, we first identified the location of ApoE in relation to fibrillary Aβ within basement membranes in the walls of arteries in AD. Secondly, we performed single-molecule force spectroscopy with an atomic force microscope (AFM) in order to determine the force of attachment between Aβ/ApoE4 complexes and the basement membrane protein, laminin. We then compared the attachment forces of Aβ/ApoE4 complexes with those of Aβ/ApoE3.

2. Materials and Methods

2.1 Materials for AFM tip functionalization

Analytical grade materials used for AFM tip functionalization were obtained from Sigma Aldrich, UK. The following chemicals were used: ethanol, chloroform, ethanolamine hydrochloride (ethanolamine-HCl), dimethylsulfoxide (DMSO), triethylamine (TEA), sodium hydroxide (NaOH), sodium cyanoborohydride ($NaCNBH_3$). Aldehyde-PEG-NHS linker was purchased from Institute of Biophysics, University of Linz, Austria. Human recombinant laminin-511 was purchased from (BioLamina, Sweden), while human Aβ40 (referred to as Aβ for the rest of the manuscript), human ApoE3 and human ApoE4 were from Cambridge Bioscience (Cambridge, UK).

2.2 Immunofluorescence of human tissue

Paraffin sections from 5 cases diagnosed with Alzheimer's disease from the South West Dementia Brain Bank, Frenchay Hospital, Bristol were utilised for immunostaining. Sections of middle frontal gyrus were immunostained with antibodies specific for Aβ42 (clone 21F12, 1:4000), pan-apolipoprotein E (pan-apoE, clone 5F6, 1:2000) provided by Elan Pharmaceuticals Inc. (USA). We could not access an antibody specific for Aβ40 that worked on human tissue, so we used Aβ42, as we know that Aβ42 becomes entrapped in the

cerebrovascular amyloid deposits [18, 19]. Smooth muscle actin (SMA: clone 1A4, Dako, UK, 1:100) was used to identify smooth muscle cells in the blood vessel walls.

Immunostaining was performed using the appropriate antigen retrieval methods for each primary antibody. For Aβ42, pan-apoE and ApoE E4 sections were pre-treated with neat formic acid. Triple immunostaining was detected using AF594 (red, Aβ42) or AF633 (blue, pan-apoE) fluorochromes conjugated with biotinylated secondary antibodies (Life Technologies, UK) and SMA-FITC (Abcam, UK, 1:200, green), respectively. A Leica SP5 confocal scanning microscope was used for imaging.

2.3 Atomic force microscope measurements

2.3.1 Functionalization of AFM measuring tips

The AFM silicon nitride tips (MSNL-10, Bruker, UK) were functionalized with the desired protein following three modification steps: (1) amino functionalization, (2) modification with aldehyde-PEG-NHS linker, and (3) ligand coupling. AFM cantilevers were washed in chloroform three times and dried under a stream of nitrogen before tips were subjected to modification. Amino functionalization was done by esterification with ethanolamine at room temperature [20]. AFM tips were then placed in a closed container with the ethanolamine-HCl solution, left overnight, washed three times in DMSO and ethanol and dried under a stream of nitrogen. Subsequent functionalization steps were performed following a custom tip modification protocol provided by Agilent Technologies, Inc. [21]. The PEG linker was immobilized on aminated AFM probes by the NHS ester terminus (step 2). 3.3 mg of aldehyde-PEG-NHS linker was dissolved in 1 ml chloroform, and transferred into a small glass reaction chamber. 10 μl of thriethylamine was added before amino-functionalized AFM tips were immersed into the solution. The chamber was covered to prevent chloroform evaporation. After 1.5 hours, tips were removed from the solution,

washed three times in chloroform, and dried under the stream of nitrogen. The use of PEG spacer, as an intermittent link for biomolecule attachment to the cantilever, provides important advantages in molecular recognition force spectroscopy [22-26]. The linker is chemically and physically inert, allowing rapid and free reorientation of biomolecules. The spacing between molecule and the tip reduces the likelihood of molecules being crushed during the probe-surface contact. Non-linear elastic properties of PEG make it easy to discriminate between the non-specific and specific interaction events.

Proteins (Laminin, ApoE3, or ApoE4) were immobilized on AFM probes using the amine-amine reactive linker aldehyde-PEG-NHS. A sheet of parafilm was pressed into a glass petri dish. AFM cantilever chips were set onto the film in a circular "wagon wheel" pattern so that the tips were pointed upward and inward. 10 - 30 μl of the protein solution was applied onto the cantilevers. The proteins were allowed to react for one hour to couple via intrinsic amino groups to the aldehyde-function of the PEG linker on the tip. After one hour, 5 μl of 1M ethanolamine was added to the protein solution drop to inactivate unreacted aldehyde groups.

2.3.2 Substrate preparation for AFM experiments

Substrates for AFM experiments were prepared as follows: 20 μl of protein solution, i.e. Aβ, ApoE3, ApoE4, or complexes of ApoE3 + Aβ (1:1 molar ratio), and ApoE4 + Aβ (1:1 molar ratio). Complexes were left to react at 4°C for 1 hour. Solutions were added onto a freshly cleaved mica (Agar Scientific, UK) substrate which was already inserted into a liquid cell. 100 μl of dH_2O were added to a cell. Proteins were left to adsorb to the substrate for 30 min. The mica substrate was washed with water to ensure that only adsorbed proteins remained on the substrate.

Aβ has a tendency to form large aggregates with time [27]. To maintain the solubility state of Aβ, fresh protein was deposited on the mica every 4 hours, and a new functionalized AFM tip was used in the experiments. Images of Aβ were captured immediately after deposition and before the possible Aβ rearrangement, i.e. after 4 hours. No Aβ agglomeration in fibrillar form was observed on the mica during any stage of the experiment.

2.3.3 Single molecule force spectroscopy experiments

Sample imaging and molecular force spectroscopy experiments were performed in water using Agilent 5500 Scanning Probe Microscopy, MAC III, Agilent Technologies, US. Images were acquired using the same cantilevers in contact mode. Actual constant values of AFM cantilevers were measured in liquid using a built-in thermal noise method [28] before each experimental set. Determined force constant was used to calculate actual loading and unbinding forces. Force spectroscopy data were acquired at loading rates ranging from 3000 – 160000 pN/s, corresponding to retraction rates of 0.08 – 3 μm/s. At least 1000 curves were recorded for each experimental condition. The following tip-substrate pairs were measured: Laminin - Aβ, Laminin - ApoE3, Laminin - ApoE4, or Laminin (on the tip), against complexes of ApoE3 + Aβ, or ApoE4 + Aβ. In a separate run of experiments, we used ApoE3 on the tip and Aβ as a substrate, or ApoE4 on the tip and Aβ as a substrate. All experiments were repeated independently three times, allowing 2 – 3 weeks between each repeat.

2.3.4 Data Analysis

PicoView 1.10 and PicoImage (Agilent Technologies, US) software were used for data acquisition and image analysis, respectively. Force curves were analysed using PUNIAS macro software (http://punias.voila.net/). From several hundred single molecule unbinding events, the probability density function (PDF) was constructed as described in [29, 30]. The PDFs were fitted with the equation:

$$p(F) = \sum_{i=1}^{N} \frac{1}{N\sigma_i\sqrt{2\pi}} exp\left(-\frac{(F-\mu_i)^2}{2\sigma_i^2}\right) \quad (1)$$

where $p(F)$ is the estimate for the PDF that the bond will break at force F, μ_i and σ_i are rupture force and accuracy respectively, with the sum running over all N (several hundred in our case) rupture events. PDF gives the statistical distribution of rupture forces (termed as "unbinding force"). The most probable unbinding force was then determined by fitting Gauss function to the estimated PDF using Origin analytical software.

In a single barrier model [31], the unbinding force F_U is given as a function of the loading rate:

$$F_U = \frac{k_B T}{x_\beta}\ln(r) - \frac{k_B T}{x_\beta}\ln\left(k_{off}\frac{k_B T}{x_\beta}\right) \quad (2)$$

where k_BT is the thermal energy (4.1 pNnm at room temperature), k_{off} (1/s) is the dissociation rate constant, x_β is a length scale in nm describing the separation of the receptor-ligand pair between the bound and the transition state, r (pN/s) is the loading rate. The parameters x_β and k_{off} were determined by fitting F_U against ln(r).

3. Results

3.1 Immunofluorescence

Aβ42 was observed in the walls of blood vessels from brains with Alzheimer's disease (Figure 1). ApoE was also observed in the walls of arteries, between the layers of smooth muscle cells and co-localized with Aβ42 (Figure 1).

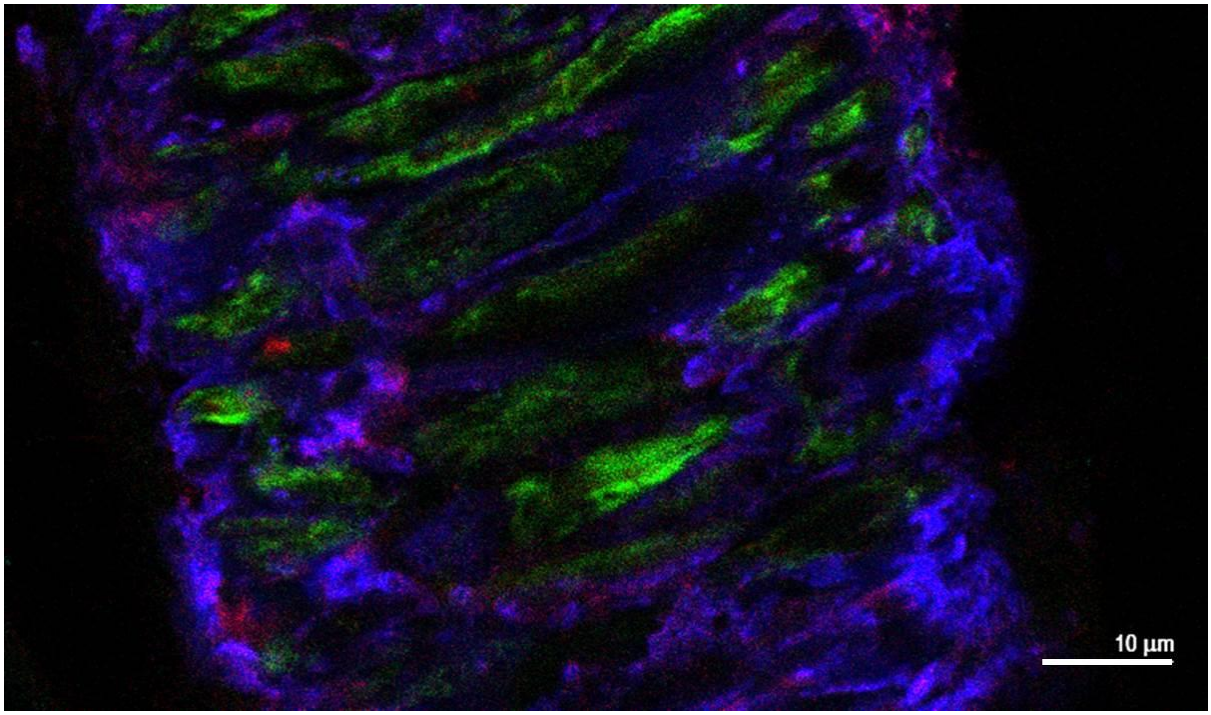

Figure 1. Triple immunostaining for Amyloid-β (Aβ) 1-42 (red), pan-Apolipoprotein E (ApoE) (blue), smooth muscle actin (green) of a leptomeningeal artery of a case of Alzheimer's disease. Aβ42 co-localizes with apolipoprotein E (magenta) adjacent to smooth muscle actin, suggesting that Aβ and ApoE co-localize in the basement membranes of the smooth muscle tunica media. Confocal Leica SP5 image, a 63 objective was used, scale bar 10 µm.

3.2 Molecule force spectroscopy

Force-spectroscopy experiments were performed to study the reciprocal influence of different isoforms of ApoE and Aβ on their binding interactions with laminin. The protein adsorption on the mica, its conformation and size was investigated by contact-mode AFM imaging in liquid. As an example, Figure 2a shows Aβ assemblies on the substrate. Scratching away adhered molecules with higher force, gave 2 x 2 μm area of bare (or almost bare) mica (Figure 2b). This simple experiment further confirmed protein presence on the surface. Furthermore, it also indicates that Aβ is in the form of small oligomers (molecules were of about 5 ± 0.5 nm in height) instead of fibrils as described in Refs. [32, 33] or large agglomerates. ApoEs were measured to be 15 ± 2 nm in height, and complexes of Aβ with ApoE3/4 were 20 ± 2 nm.

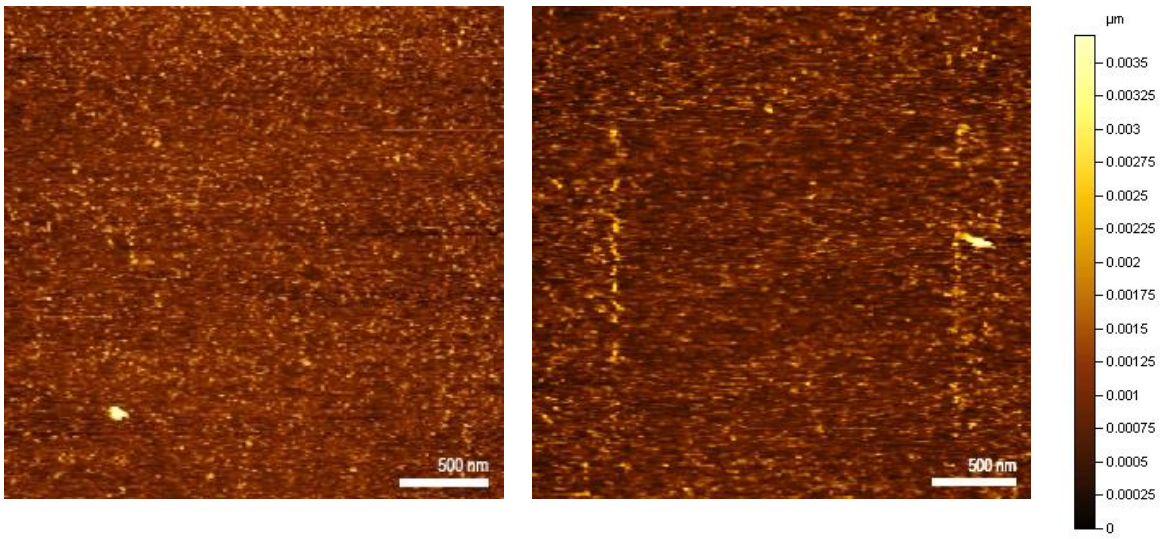

(a) (b)

Figure 2. Contact-mode AFM images in liquid of Aβ deposited on mica (a). The presence of protein molecules was proved by scratching the proteins with higher force in an area of 2 x 2 μm (b). Scale bar – 500 nm.

To study specific binding of tip-bound protein to mica-bound protein by force spectroscopy, the functionalized tip was repeatedly brought into contact with the protein and retracted at constant load and velocity. Figure 3a shows an example of typical force-distance curve with a single recognition event. The cycle starts at a point 1 which corresponds to the free cantilever, when the tip is far away from the substrate. The probe comes in contact with the surface at point 2, and bends further until it reaches point 3. During unloading, the cantilever relaxes to reach point 4, which usually corresponds to the point of contact. If there is specific interaction between biomolecules, the unloading curve follows the pass through steps 5-7. The cantilever begins to deflect in a non-linear fashion. This characteristic signature peak results from the stretching of the polymer linker, and identifies specific ligand-receptor binding. The force increases until enough energy is transferred to break the bond (points 6 to 7), where F_U indicates an unbinding force in pN. The tip and substrate are completely separated at this point. To ensure that the measured unbinding event is specific to the ligand-receptor interaction, the force-displacement curves between the functionalized tip and clean mica in an aqueous environment were recorded. As expected, all loading and unloading curves were identical in control experiments, Figure 3b.

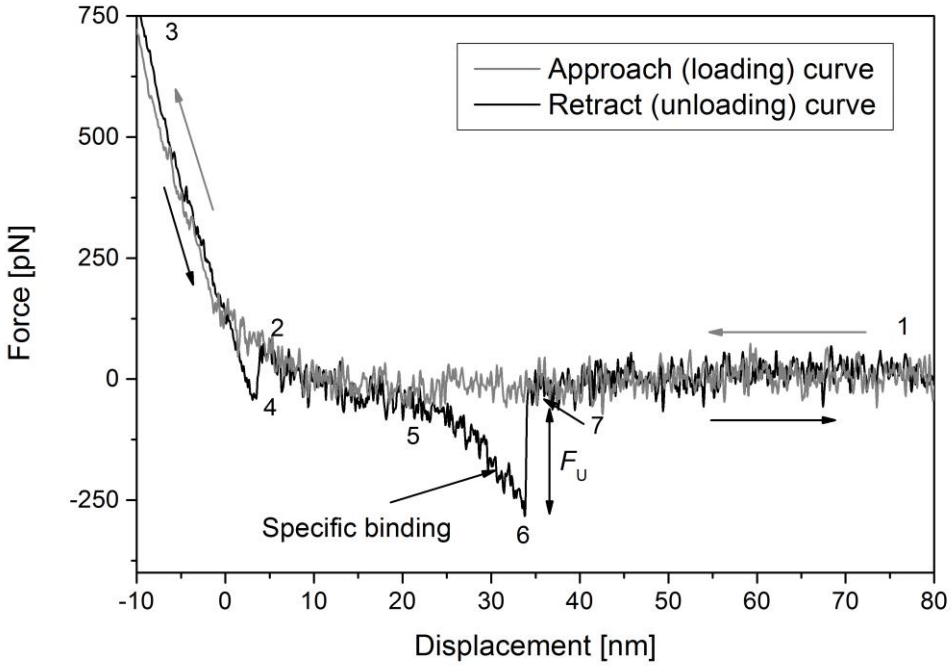

(a)

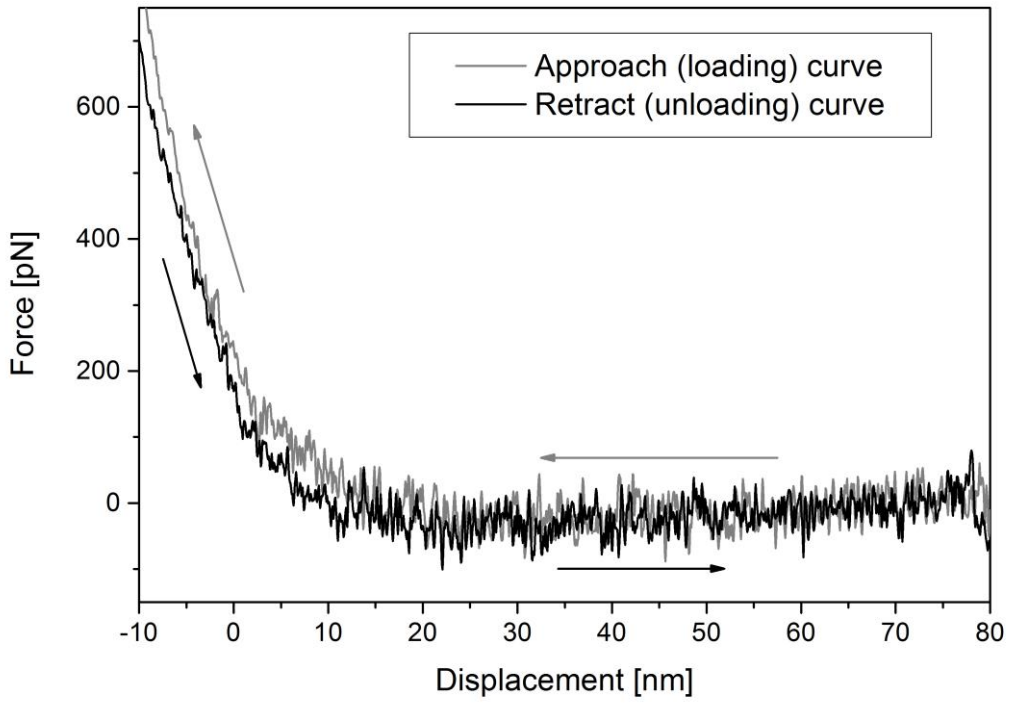

(b)

Figure 3. Example of force-displacement curves obtained during single molecule force spectroscopy experiments for an experimental set tip - ApoE3, substrate - Aβ. (a) Typical force-displacement cycle with a single specific interaction. See text for explanation. (b) Control - no interaction between biomolecules attached to the tip and clean mica substrate.

Force-displacement cycles were analysed as described in materials and methods. The most probable unbinding force and binding probabilities (BP) were calculated using Equations 1 and 2. The F_U and binding probability results for various ligand-receptor pairs recorded at 1 Hz with 100-300 nm amplitude, resulting in loading rates from 15,000 – 70,000 pN/s, are presented in Figure 4. The unbinding forces between laminin and ApoE3 and between laminin and apoE4 are the same (450 ± 50 pN), Figure 4a. However, when Aβ was added to ApoE, less energy was required to detach a laminin molecule from any of the complexes (~ 270 ± 25 pN). It was also noted that unbinding of ApoE3 and ApoE4 from Aβ occurred with similar force of ~ 270 ± 25 pN, while laminin bonded to Aβ at forces of 350 ± 35 pN.

The binding probability was defined as the probability of recording an unbinding event in a force-distance cycle in relation to all recorded cycles, i.e. how many curves with specific recognition were recorded out of 1000 measured cycles. Results of binding probability for various tip-substrate interaction are given in Figure 4b, where BP of 1 would correspond to 100%, 0.3 = 30%, and so on. Laminin tended to bind more frequently to ApoE3, Aβ, and Aβ+ApoE3 complex with a probability of ~ 30 ± 3%. BP of laminin to ApoE4 was calculated to be 15 ± 1.5 %, and for Aβ+ApoE4 complex it was 22 ± 2 %. Very few binding events were recorded between ApoE3/4 (tip) and Aβ (substrate), where 7% of all specific recognition curves were recorded for ApoE4 - Aβ interaction, and 2% for ApoE4 - Aβ (Figure 4b, grey columns). Aβ was always immobilized on the mica, and so the protein orientation might have been such that binding sites were directed towards the substrate leaving very few sites exposed. In this case, ApoEs attached to the AFM tip would hardly bind to Aβ. If this were the case, similar results should be observed between laminin (tip) and Aβ (substrate). But experimental binding probability between laminin and Aβ was 30%, and so this would indicate that ApoEs do not interact with Aβ so avidly.

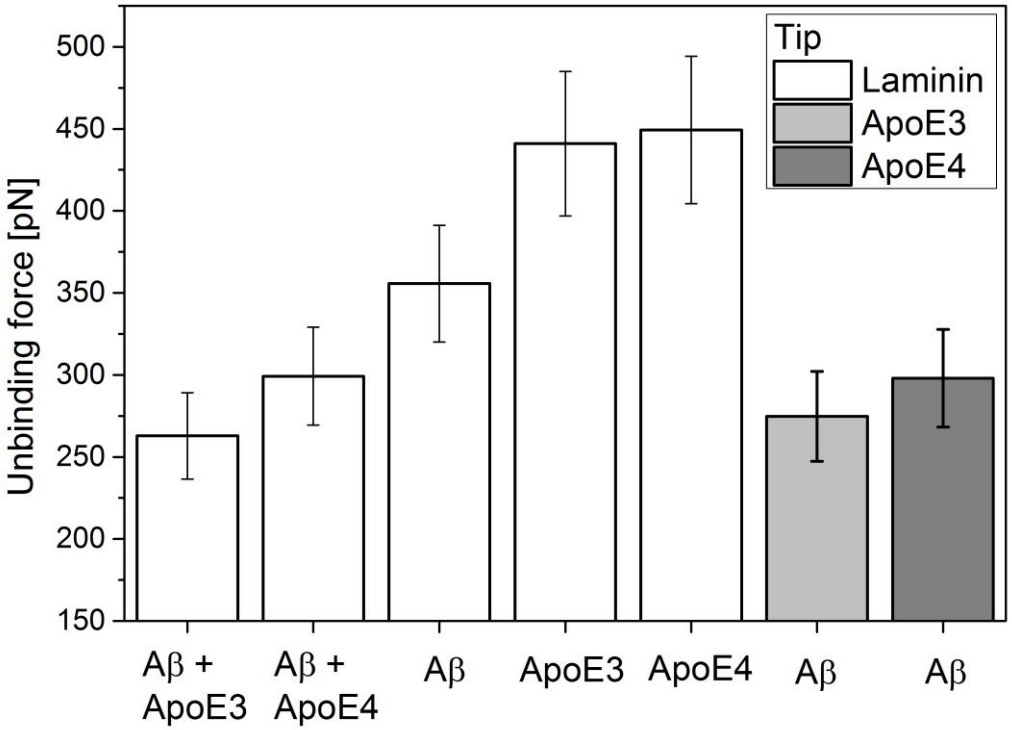

(a)

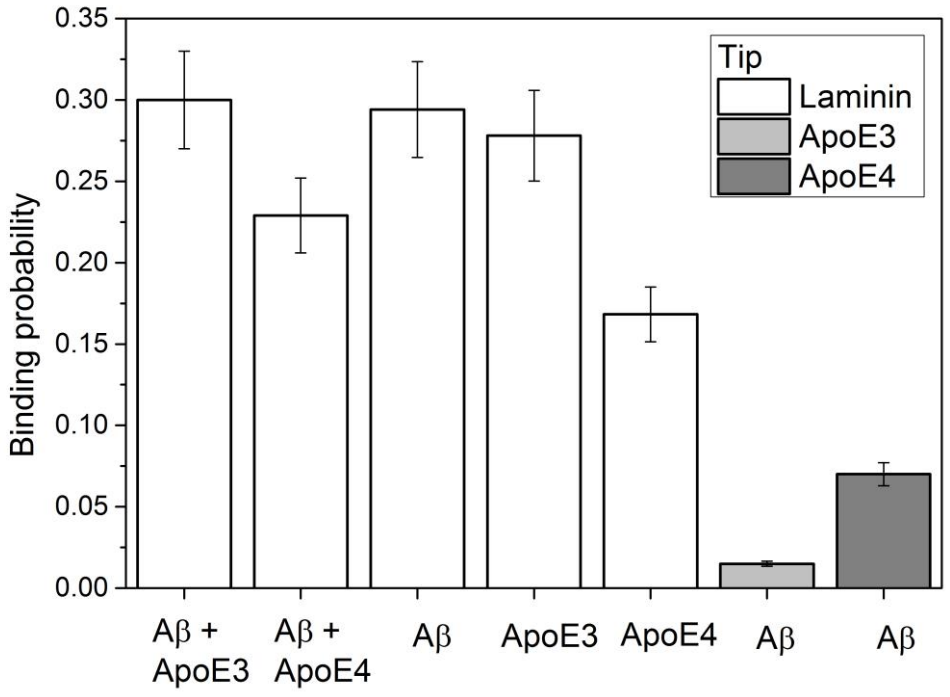

(b)

Figure 4. (a) Most probable unbinding force, F_U, and (b) specific binding probability for various tip-substrate pairs. Results are given for force-displacement cycles obtained at 1 Hz with 100 – 300 nm amplitude.

3.3 Kinetic constants and affinities

The parameters of prime interest in describing any biological ligand-receptor system are the rates of spontaneous association (or on-rate, k_{on}), dissociation (off-rate, k_{off}), and their ratio the dissociation constant (also known as affinity) $K_D = k_{off}/k_{on}$ which describes the equilibrium behaviour. To calculate association and dissociation constants, molecular force spectroscopy experiments were carried out in a range of loading rates from 3000 – 160000 pN/s, and tip-substrate contact times 0.001 – 0.5 s. To estimate kinetic on-rate constant, k_{on}, from single molecule unbinding force measurements, it is necessary to determine interaction time τ (the time required for half maximal recognition probability) and effective concentration c_{eff}, for $k_{on} = (\tau\, c_{eff})^{-1}$[23, 34, 35]. The effective concentration is described as a number of binding receptor molecules within the effective volume accessible for free equilibrium interaction, and is explained in detail elsewhere [23, 34, 35]. The interaction time was calculated from the binding probability at different encounter times by fitting $P = A(1 - \exp(-(t - t_0)/\tau))$ (where t_0 is a lag time, A is the maximum observable binding probability) [34]. An example is shown in figure Figure 5(a) for ApoE4 interaction with Aβ.

Furthermore, according to single barrier theory, the unbinding force rises linearly with respect to logarithmically increasing loading rate [30, 36, 37]. A linear increase of the most probable unbinding force versus loading rate was observed for all measured interactions. As an example, Figure 5(b) demonstrates unbinding force dependence on loading rate for ApoE4 interaction with Aβ. The off-rate is determined from the linear fit extrapolated at zero force [36, 37]. The slope of the fit corresponds to $k_\beta T/x_\beta$ in Equation 2. The intercept at zero force allows the calculation of k_{off} from Equation 2, $\left(-\frac{k_\beta T}{x_\beta} ln\left(k_{off}\frac{k_\beta T}{x_\beta}\right)\right)$.

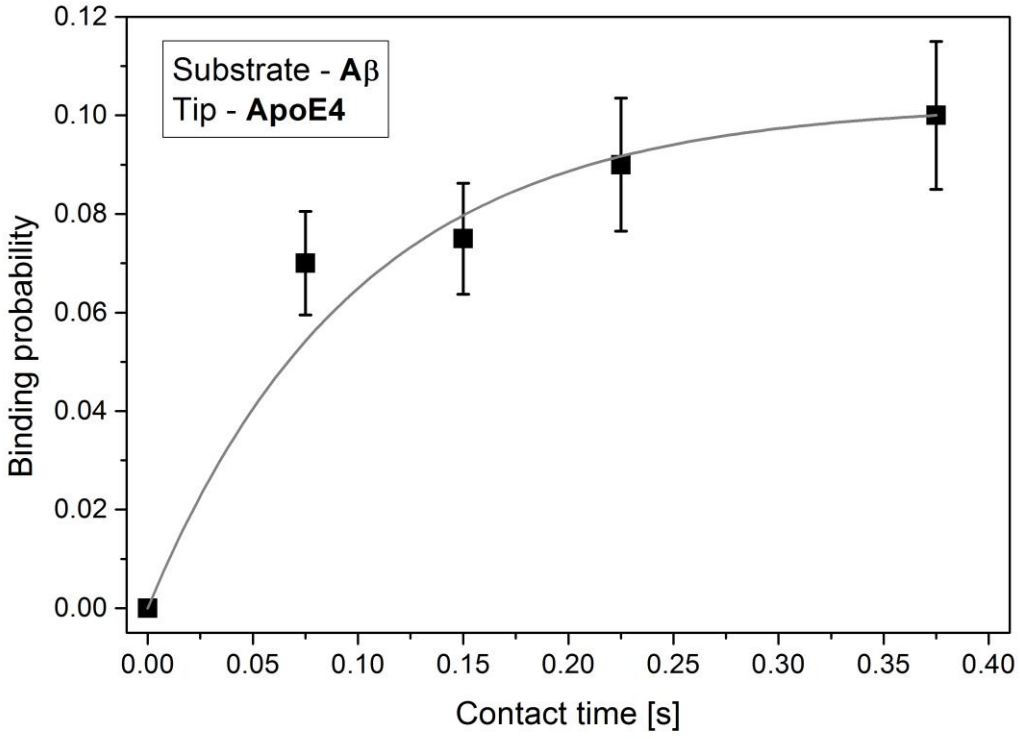

(a)

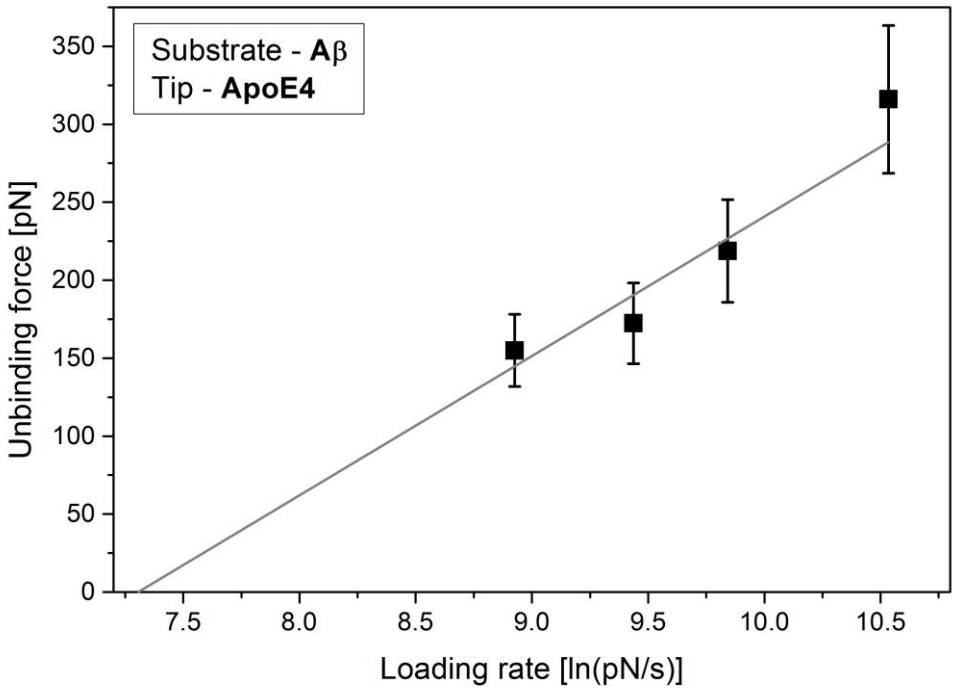

(b)

Figure 5. Kinetics of ligand-receptor binding. (a) Binding probability as a function of contact time. Solid line is the result of least- squares fit. (b) Unbinding force as a function of loading rate.

Calculated rate constants and affinities for all AFM measured ligand-receptor pairs is given in Table 1. The results for all AFM measurements demonstrate that Aβ + ApoE3 complex has a stronger binding to laminin than Aβ + ApoE4.

Table 1. Association (k_{on}) and dissociation (k_{off}) rates, and affinity (K_D) obtained by AFM. The lower K_D value indicates stronger interaction. Aβ + ApoE3 has a stronger binding to laminin, compared to Aβ + ApoE4.

Tip	Substrate	k_{on} (1/Ms)	k_{off} (1/s)	K_D (1/M)
ApoE3	Aβ	2.26×10^{4}	0.01091	4.83×10^{-7}
ApoE4	Aβ	1.08×10^{5}	0.01025	9.45×10^{-8}
Laminin	Aβ	1.10×10^{6}	0.01241	1.13×10^{-8}
	ApoE3	2.08×10^{6}	0.00541	2.60×10^{-9}
	ApoE4	1.07×10^{6}	0.00527	4.94×10^{-9}
	Aβ + ApoE3	1.23×10^{6}	0.018	1.46×10^{-8}
	Aβ + ApoE4	1.46×10^{5}	0.02224	1.52×10^{-7}

4. Discussion

The results of the present study have shown that ApoE and Aβ42 co-localize within basement membranes of the cerebral vasculature that form the elimination pathways for Aβ from the brain, consistent with Aβ being eliminated from the brain as a complex with ApoE [12]. Electron paramagnetic resonance spectroscopy study of the interactions between

apolipoprotein E and oligomers of Aβ40 demonstrate that ApoE3 has a higher affinity for Aβ40 compared to ApoE4 [38]. Our own data show stronger binding of Aβ40 to ApoE4 compared with ApoE3. Other studies have shown that ApoE4 binds Aβ with higher affinity compared with ApoE3 and this is reversed when using lipidated forms of ApoE [39, 40] . More recently, using HEK-293 cells expressing ApoE3 or ApoE4 and Aβ42 it was shown that the interactions between ApoE4 and Aβ42 are weaker compared with ApoE3- Aβ42, with ApoE3-Aβ complexes saturable and dependent on Aβ concentrations [41]. We did not use Aβ42 in this study, but Aβ40, the type predominantly found in the walls of blood vessels and we used a ratio of Aβ-ApoE of 1:1, as our aim was to concentrate on the interaction of the Aβ40-ApoE3/4 complexes with the laminin component of the basement membranes.

We found that the complex Aβ + ApoE4 interacted with laminin less avidly (K_D = 1.52 x 10^{-7} M^{-1}) compared to the complex Aβ + ApoE3 (K_D = 1.46 x 10^{-8} M^{-1}). These results, together with our mathematical modelling studies (4), suggest that the perivascular clearance of soluble Aβ along cerebrovascular basement membranes may be slower in ApoE4 carriers, compared to ApoE3 carriers, due to a lack of biophysical interaction between Aβ and individual components of basement membranes (in this case laminin). Less efficient biophysical interaction between Aβ + ApoE4 and basement membrane proteins, such as laminin would mean that there would be weaker attachment to the basement membrane during passage of the pulse wave and ApoE4-Aβ complexes may remain in the extracellular spaces as seeds for plaques, promoting inflammation [42, 43]. Thus Aβ + ApoE4 would not be driven out of the brain along perivascular pathways as efficiently as Aβ + ApoE3. This may be an important factor in the failure of elimination of Aβ from the brain in ApoE4 carriers and the consequent accumulation of Aβ in the brain and artery walls and the development of Alzheimer's disease. Apolipoprotein E appears to be located in the

perivascular compartment of blood vessels in the human brain and co-localizes with Aβ in Alzheimer's disease [44].

Elimination of Aβ from the brain in Alzheimer's disease has been the major objective of a number of Aβ immunotherapy trials. Although in many patients insoluble plaques of Aβ are cleared from cortical areas, an increase in the severity of CAA has been reported [45]. This suggests that Aβ cleared from the brain parenchyma becomes entrapped in the perivascular drainage pathways with the ultimate failure of elimination of Aβ from the brain [45]. Recently it has also been demonstrated that Aβ immunotherapy was associated with redistribution of ApoE from cortical plaques to cerebral vessel walls, mirroring the altered distribution of Aβ 42 from the plaques towards the walls of blood vessels [46], consistent with ApoE/Aβ travelling as a complex. Complications are associated with Aβ immunotherapy, designated Amyloid Related Imaging Abnormalities (ARIA) [47]. Evidence suggests that ARIAs are due to vascular alterations, including increased severity of CAA. As ARIAs occur more frequently in AD patients who are *APOE* ε4 carriers than non-ε4 carriers, the differential binding of Aβ/apoE E3 and E4 to laminin demonstrated in this study may be relevant to the causation of ARIA as Aβ is being removed from the brain.

5. Conclusions

The results of this study add to our knowledge of the dynamics of perivascular drainage and its importance for the elimination of Aβ from the brain. Accumulation of soluble and insoluble Aβ in brain parenchyma and in artery walls occurs with advancing age and is enhanced in those possessing the ApoE4 allele. Experimental and theoretical data indicate that vascular pulsations are the driving force for perivascular elimination of Aβ with the contrary (reflection) wave driving Aβ and other solutes out of the brain in the reverse

direction to blood flow [11]. Reduction in the amplitude of the pulse wave may occur as arteries stiffen with age and arteriosclerosis, thus reducing the motive force for the perivascular drainage of Aβ and other solutes from the brain.

The present study suggests that the presence of ApoE4 further reduces the efficiency of perivascular elimination of Aβ due to reduced attachment of ApoE4/Aβ complexes to basement membranes in the drainage pathway, although the type of Aβ and the lipidation status of ApoE are crucial [12]. Such reduced attachment may allow oscillation of Aβ within the basement membrane during passage of the pulse wave and thus impair the progress of Aβ out of the brain along the perivascular pathways.

Therapeutic strategies that optimise attachment of soluble metabolites to basement membrane proteins may also optimise elimination of those metabolites from the brain. The present study has established a principle that could be developed in the future to test therapies for the prevention of Alzheimer's disease, based on manipulating the Aβ-ApoE interactions with basement membrane proteins.

Acknowledgements

We are grateful to Cheryl Hawkes for technical help, to the Engineering and Physical Sciences Research Council of UK and Alzheimer's Research UK for providing the funding for this study, to the South West Dementia Brain Bank for the brain tissue.

References

[1] D.R. Thal, W.S.T. Griffin, R.A.I. de Vos, E. Ghebremedhin, Cerebral amyloid angiopathy and its relationship to Alzheimer's disease, Acta Neuropathol, 115 (2008) 599-609.

[2] D.R. Thal, A. Papassotiropoulos, T.C. Saido, W.S.T. Griffin, R.E. Mrak, H. Kolsch, K. Del Tredici, J. Attems, E. Ghebremedhin, Capillary cerebral amyloid angiopathy identifies a

distinct APOE epsilon 4-associated subtype of sporadic Alzheimer's disease, Acta Neuropathol, 120 (2010) 169-183.

[3] R.O. Carare, C.A. Hawkes, M. Jeffrey, R.N. Kalaria, R.O. Weller, Review: Cerebral amyloid angiopathy, prion angiopathy, CADASIL and the spectrum of protein elimination failure angiopathies (PEFA) in neurodegenerative disease with a focus on therapy, Neuropath Appl Neuro, 39 (2013) 593-611.

[4] R. Deane, A. Sagare, K. Hamm, M. Parisi, S. Lane, M.B. Finn, D.M. Holtzman, B.V. Zlokovic, apoE isoform-specific disruption of amyloid beta peptide clearance from mouse brain, J Clin Invest, 118 (2008) 4002-4013.

[5] R.O. Weller, M. Subash, S.D. Preston, I. Mazanti, R.O. Carare, Perivascular drainage of amyloid-beta peptides from the brain and its failure in cerebral amyloid angiopathy and Alzheimer's disease, Brain Pathol, 18 (2008) 253-266.

[6] I. Szentistvanyi, C.S. Patlak, R.A. Ellis, H.F. Cserr, Drainage of Interstitial Fluid from Different Regions of Rat-Brain, Am J Physiol, 246 (1984) F835-F844.

[7] R.O. Carare, M. Bernardes-Silva, T.A. Newman, A.M. Page, J.A.R. Nicoll, V.H. Perry, R.O. Weller, Solutes, but not cells, drain from the brain parenchyma along basement membranes of capillaries and arteries: significance for cerebral amyloid angiopathy and neuroimmunology, Neuropath Appl Neuro, 34 (2008) 131-144.

[8] Y. Shinkai, M. Yoshimura, Y. Ito, A. Odaka, N. Suzuki, K. Yanagisawa, Y. Ihara, Amyloid P-Proteins-1-40 and P-Proteins-1-42(43) in the Soluble Fraction of Extracranial and Intracranial Blood-Vessels, Ann Neurol, 38 (1995) 421-428.

[9] C.A. Hawkes, W. Hartig, J. Kacza, R. Schliebs, R.O. Weller, J.A. Nicoll, R.O. Carare, Perivascular drainage of solutes is impaired in the ageing mouse brain and in the presence of cerebral amyloid angiopathy, Acta Neuropathol, 121 (2011) 431-443.

[10] C.A. Hawkes, P.M. Sullivan, S. Hands, R.O. Weller, J.A.R. Nicoll, R.O. Carare, Disruption of Arterial Perivascular Drainage of Amyloid-beta from the Brains of Mice Expressing the Human APOE epsilon 4 Allele, Plos One, 7 (2012).

[11] D. Schley, R. Carare-Nnadi, C.P. Please, V.H. Perry, R.O. Weller, Mechanisms to explain the reverse perivascular transport of solutes out of the brain, J Theor Biol, 238 (2006) 962-974.

[12] L.M. Tai, S. Mehra, V. Shete, S. Estus, G.W. Rebeck, G.J. Bu, M.J. LaDu, Soluble apoE/A beta complex: mechanism and therapeutic target for APOE4-induced AD risk, Mol Neurodegener, 9 (2014).

[13] S.R. Li, K. Oka, D. Galton, J. Stocks, Bst-1 Rflp at the Human Lipoprotein-Lipase (Lpl) Gene Locus, Nucleic Acids Res, 16 (1988) 11856-11856.

[14] S.R. Li, K. Oka, D. Galton, J. Stocks, Pvu-Ii Rflp at the Human Lipoprotein-Lipase (Lpl) Gene Locus, Nucleic Acids Res, 16 (1988) 2358-2358.

[15] D.R. Riddell, H. Zhou, K. Atchison, H.K. Warwick, P.J. Atkinson, J. Jefferson, L. Xu, S. Aschmies, Y. Kirksey, Y. Hu, E. Wagner, A. Parratt, J. Xu, Z.T. Li, M.M. Zaleska, J.S. Jacobsen, M.N. Pangalos, P.H. Reinhart, Impact of Apolipoprotein E (ApoE) Polymorphism on Brain ApoE Levels, J Neurosci, 28 (2008) 11445-11453.

[16] P.B. Verghese, J.M. Castellano, K. Garai, Y.N. Wang, H. Jiang, A. Shah, G.J. Bu, C. Frieden, D.M. Holtzman, ApoE influences amyloid-beta (A beta) clearance despite minimal

apoE/A beta association in physiological conditions, P Natl Acad Sci USA, 110 (2013) E1807-E1816.

[17] M.C. Herzig, W.E. Van Nostrand, M. Jucker, Mechanism of cerebral beta-amyloid angiopathy: Murine and cellular models, Brain Pathol, 16 (2006) 40-54.

[18] J. Nicoll, The effects of A beta immunization on the pathology of Alzheimer disease, Neurobiol Aging, 27 (2006) S15-S15.

[19] J.A.R. Nicoll, E. Barton, D. Boche, J.W. Neal, I. Ferrer, P. Thompson, C. Vlachouli, D. Wilkinson, A. Bayer, D. Games, P. Seubert, D. Schenk, C. Holmes, A beta species removal after A beta(42) immunization, J Neuropath Exp Neur, 65 (2006) 1040-1048.

[20] C.K. Riener, C.M. Stroh, A. Ebner, C. Klampfl, A.A. Gall, C. Romanin, Y.L. Lyubchenko, P. Hinterdorfer, H.J. Gruber, Simple test system for single molecule recognition force microscopy, Analytica Chimica Acta, 479 (2003) 59-75.

[21] Agilent Technologies PicoTREC Topography and Recognition Imaging System, User's Guide in, Agilent technologies, Inc., 2010.

[22] A. Ebner, P. Hinterdorfer, H.J. Gruber, Comparison of different aminofunctionalization strategies for attachment of single antibodies to AFM cantilevers, Ultramicroscopy, 107 (2007) 922-927.

[23] P. Hinterdorfer, W. Baumgartner, H.J. Gruber, K. Schilcher, H. Schindler, Detection and localization of individual antibody-antigen recognition events by atomic force microscopy, Proceedings of the National Academy of Sciences of the United States of America, 93 (1996) 3477-3481.

[24] V.J. Morris, Kirby, A.R., Gunning, A.P., Force spectroscopy, in: Atomic Force Microscopy for Biologist, Imperila College Press, 2010, pp. 356-396.

[25] G.S. Watson, Watson, J.A., Quantitative measurements of nano forces using Atomic Force Microscopy, VDM Verlag Dr. Muelller, 2008.

[26] W.F. Heinz, J.H. Hoh, Spatially resolved force spectroscopy of biological surfaces using the atomic force microscope, Trends in Biotechnology, 17 (1999) 143-150.

[27] D.R. Thal, M. Fandrich, Protein aggregation in Alzheimer's disease: A beta and tau and their potential roles in the pathogenesis of AD, Acta Neuropathol, 129 (2015) 163-165.

[28] J.L. Hutter, J. Bechhoefer, Calibration of Atomic-Force Microscope Tips, Review of Scientific Instruments, 64 (1993) 1868-1873.

[29] W. Baumgartner, P. Hinterdorfer, H. Schindler, Data analysis of interaction forces measured with the atomic force microscope, Ultramicroscopy, 82 (2000) 85-95.

[30] C. Rankl, F. Kienberger, H. Gruber, D. Blaas, P. Hinterdorfer, Accuracy estimation in force spectroscopy experiments, Japanese Journal of Applied Physics Part 1-Regular Papers Brief Communications & Review Papers, 46 (2007) 5536-5539.

[31] E. Evans, K. Ritchie, Dynamic strength of molecular adhesion bonds, Biophysical Journal, 72 (1997) 1541-1555.

[32] L.M. Jungbauer, C. Yu, K.J. Laxton, M.J. Ladu, Preparation of fluorescently-labeled amyloid-beta peptide assemblies: the effect of fluorophore conjugation on structure and function, J Mol Recognit, 22 (2009) 403-413.

[33] J.D. Harper, S.S. Wong, C.M. Lieber, P.T. Lansbury, Assembly of A beta amyloid protofibrils: An in vitro model for a possible early event in Alzheimer's disease, Biochemistry, 38 (1999) 8972-8980.

[34] C. Rankl, F. Kienberger, L. Wildling, J. Wruss, H.J. Gruber, D. Blaas, P. Hinterdorfer, Multiple receptors involved in human rhinovirus attachment to live cells, Proceedings of the National Academy of Sciences of the United States of America, 105 (2008) 17778-17783.

[35] W. Baumgartner, Gruber, H.J., Hinterdorfer, P., Drenckhahn, D., Affinity of trans-interacting VE-candherin determined by atomic force microscopy, Single Molecules, 1 (2000) 119-122.

[36] F. Schwesinger, R. Ros, T. Strunz, D. Anselmetti, H.J. Guntherodt, A. Honegger, L. Jermutus, L. Tiefenauer, A. Pluckthun, Unbinding forces of single antibody-antigen complexes correlate with their thermal dissociation rates, Proceedings of the National Academy of Sciences of the United States of America, 97 (2000) 9972-9977.

[37] T. Strunz, K. Oroszlan, R. Schafer, H.J. Guntherodt, Dynamic force spectroscopy of single DNA molecules, Proceedings of the National Academy of Sciences of the United States of America, 96 (1999) 11277-11282.

[38] J. Petrlova, H.S. Hong, D.A. Bricarello, G. Harishchandra, G.A. Lorigan, L.W. Jin, J.C. Voss, A differential association of Apolipoprotein E isoforms with the amyloid-beta oligomer in solution, Proteins, 79 (2011) 402-416.

[39] M.J. Ladu, M.T. Falduto, A.M. Manelli, C.A. Reardon, G.S. Getz, D.E. Frail, Isoform-Specific Binding of Apolipoprotein-E to Beta-Amyloid, J Biol Chem, 269 (1994) 23403-23406.

[40] M.J. Ladu, T.M. Pederson, D.E. Frail, C.A. Reardon, G.S. Getz, M.T. Falduto, Purification of Apolipoprotein-E Attenuates Isoform-Specific Binding to Beta-Amyloid, J Biol Chem, 270 (1995) 9039-9042.

[41] L.M. Tai, T. Bilousova, L. Jungbauer, S.K. Roeske, K.L. Youmans, C.J. Yu, W.W. Poon, L.B. Cornwell, C.A. Miller, H.V. Vinters, L.J. Van Eldik, D.W. Fardo, S. Estus, G.J. Bu, K.H. Gylys, M.J. LaDu, Levels of Soluble Apolipoprotein E/Amyloid-beta (A beta) Complex Are Reduced and Oligomeric A beta Increased with APOE4 and Alzheimer Disease in a Transgenic Mouse Model and Human Samples, J Biol Chem, 288 (2013) 5914-5926.

[42] G.A. Rodriguez, L.M. Tai, M.J. LaDu, G.W. Rebeck, Human APOE4 increases microglia reactivity at A beta plaques in a mouse model of A beta deposition, J Neuroinflamm, 11 (2014).

[43] L.M. Tai, S. Ghura, K.P. Koster, V. Liakaite, M. Maienschein-Cline, P. Kanabar, N. Collins, M. Ben-Aissa, A.Z. Lei, N. Bahroos, S.J. Green, B. Hendrickson, L.J. Van Eldik, M.J. LaDu, APOE-modulated A beta-induced neuroinflammation in Alzheimer's disease: current landscape, novel data, and future perspective, J Neurochem, 133 (2015) 465-488.

[44] S. Utter, I.Y. Tamboli, J. Walter, A.R. Upadhaya, G. Birkenmeier, C.U. Pietrzik, E. Ghebremedhin, D.R. Thal, Cerebral small vessel disease-induced apolipoprotein E leakage is associated with Alzheimer disease and the accumulation of amyloid beta-protein in perivascular astrocytes, J Neuropath Exp Neur, 67 (2008) 842-856.

[45] D. Boche, C. Holmes, D. Wilkinson, V. Hopkins, A. Bayer, R. Jones, R. Bullock, S. Love, J. Neal, G. Yadegarfar, E. Zotova, J.A.R. Nicoll, Continued progression of neurodegeneration in Alzheimer's disease despite complete removal of the A beta plaques?, Neuropath Appl Neuro, 34 (2008) 1-1.

543 [46] K. Sakai, D. Boche, R. Carare, D. Johnston, C. Holmes, S. Love, J.A.R. Nicoll, A beta
544 immunotherapy for Alzheimer's disease: effects on apoE and cerebral vasculopathy, Acta
545 Neuropathol, 128 (2014) 777-789.

546 [47] D.J. Werring, R. Sperling, Inflammatory cerebral amyloid angiopathy and amyloid-
547 modifying therapies: Variations on the Same ARIA?, Ann Neurol, 73 (2013) 439-441.